arXiv:1212.1551v1 [cond-mat.dis-nn] 7 Dec 2012

From microstructural features to effective toughness in disordered brittle solids

Vincent Démery,[1, *] Laurent Ponson,[1, †] and Alberto Rosso[2, ‡]
[1] *Institut Jean Le Rond d'Alembert, CNRS and UPMC Université Paris 6, UMR 7190, F-75005 Paris, France, EU*
[2] *Laboratoire Physique Théorique et Modèles Statistiques (UMR CNRS 8626),*
Université de Paris-Sud, Orsay Cedex, France, EU

The relevant parameters at the microstructure scale that govern the macroscopic resistance of heterogeneous materials are investigated theoretically. Focusing on brittle failure of disordered solids modeled as the propagation of a crack front in a random medium, our study reveals two regimes: in the collective pinning regime, the critical failure load can be expressed as a function of a few parameters only that can be extracted from the material microstructural features; in the individual pinning regime, the passage from micro to macroscale is more subtle and the full distribution of local toughness is required to be predictive. Such a rationalization of the disorder induced toughening in brittle failure open new perspectives for the design of stronger materials.

Bridging microscale properties of material with their effective behavior at the macroscale is a major challenge in both pure and applied science. In systems like brittle solids [1], ferromagnets [2, 3], superconductors [4], martensitic solids [5], etc. impurities or defects present at the microstructure scale can produce dramatic effects at the macroscopic scale, and sometimes have interesting benefits; for example large precipitate particles trap dislocations in metallic alloys, increasing notably their overall strength [6].

In this study, we address the challenge of determining the effective toughness of brittle solids in presence of disorder, like randomly distributed defects or impurities. Roux *et al.* have proposed a homogenization procedure that predicts the shape of the distribution of macroscopic toughness [7, 8]. However, it does not give any hint on the actual value of the effective toughness and its relationship with microstructural parameters. More recently, this problem has been addressed in the context of thin film peeling [9]. It was shown that periodic arrangements of strong impurities could dramatically affect the peeling front behavior and increase the overall adhesive performance. However, the case of a random distribution of heterogeneities remains largely unexplored.

Our study reveals two regimes, depending on the disorder strength. Strongly disordered materials are in the *individual pinning* regime, and their behavior depends on many microscopic parameters. On the other hand, the *collective pinning* regime occurs for weaker disorder; the effective toughness then depends on a few measurable microscopic parameters and can be predicted.

A microscopic description of a crack is in general a very complex problem involving dissipative mechanisms such as damage and non-linear processes resulting from the high level of stress near the crack tip. A major simplification occurs for cracks propagating in so-called brittle solids where the typical length scale associated with these dissipative mechanisms is much smaller than the typical size of the microstructural features in the material. Under this condition, a crack can be described as a front line propagating through quenched heterogeneities [10–12], as shown in Fig. 1. The crack dynamics is then governed by two ingredients: the material elasticity that tends to keep the front flat and the impurities that attract or repel the front. More quantitatively, a crack front $u(r,t)$ in a material with fluctuating local toughness $f(r,u)$ submitted to the external loading f_{ext} follows the evolution equation

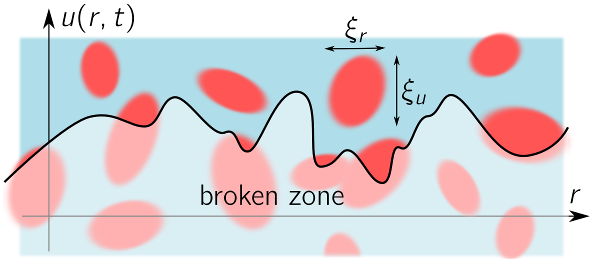

FIG. 1: (Color online) Representation of a crack front moving upwards in a disordered medium: dark red stands for high resistance areas, and light blue for low resistance areas. The defects have characteristic sizes ξ_r and ξ_u in the r and u directions, respectively.

$$\frac{\partial u}{\partial t}(r,t) = f_{\mathrm{ext}} + \frac{c}{\pi}\int \frac{u(r',t)-u(r,t)}{(r'-r)^2}dr' - f(r,u(r,t)). \tag{1}$$

The elastic constant c of the line equals the driving force f_{ext}. The long range elasticity follows from [13] and also describes the elastic energy of a wetting front [14]. Large front perturbations would require non linear corrections [15, 16], the effect of which will be neglected here.

For a random toughness field $f(r,u)$, brittle failure belongs to the wide class of disordered elastic systems, that also embraces domain walls in magnetic thin films [17] or contact lines during wetting of solids by liquids [18–20]. In these systems, a complex energy landscape with many metastable states emerges from the competition between disorder and elasticity. If the applied force f_{ext} is small, the crack front line remains pinned by the heterogeneities. When the drive exceeds a threshold value f_c, the line unpins and acquires a non-zero asymptotic velocity [21].

To describe this behavior, it has been particularly fruitful to consider the depinning transition as a regular critical phenomenon, with the velocity playing the role of an order parameter [22]. The analogy with equilibrium critical phenomena suggests that close to f_c, the front displays universal behavior with critical exponents and scaling laws that have been extensively investigated [23–26]. If the test of these predictions on experimental examples has been rather successful [27–29], the most relevant quantity from an applied science perspective is the value of depinning threshold f_c. Analogously to the critical temperature in equilibrium phase transition, the value of f_c is not universal and depends, to some extent, on the microscopic details of the system. The key point is how many and what features at the microscopic scale contribute in determining the value of the critical force.

In engineered composites, the mechanical properties of each phase and their concentration allow for the quantitative characterization of the microstructural disorder. For natural materials, high resolution microscopy techniques allow for the calculation of the toughness correlator $C(\delta r, \delta u) = \langle f(r,u) f(r+\delta r, u+\delta u)\rangle - \langle f\rangle^2$ that will be shown to provide the relevant microscopic parameters; $\langle\cdot\rangle$ denotes the average over space coordinates (r,u). From a theoretical perspective, the material microstructure is modeled by rectangular domains of constant toughness. Their length is ξ_r in the r direction; in the u direction, it is drawn in an exponential distribution of average ξ_u. On each domain, the disorder is $f = \langle f\rangle + \sigma F$, where F is drawn from a symmetric probability distribution $P(F)$ of unit variance and zero mean value. Since there is no correlation between the disorder of adjacent domains, the toughness correlator follows $C(\delta r, \delta u) = \sigma^2 \max\left(1 - \frac{r}{\xi_r}, 0\right) e^{-|\delta u|/\xi_u}$, representative of the behavior of most materials. The disorder is thus completely described by the three parameters σ, ξ_r and ξ_u and the probability distribution $P(F)$. The average toughness $\langle f\rangle$ can be absorbed in the external force and does not play any role in the study of Eq. (1).

Using the symmetries of (1), or alternatively a dimensional analysis, we can show that for a given disorder distribution $P(F)$, the dimensionless disorder parameter

$$\Sigma = \frac{\sigma \xi_r}{c \xi_u} \qquad (2)$$

allows us to write explicitly the observables dependence on the microscopic parameters:

$$B(r) = \left(\frac{\sigma \xi_r}{c}\right)^2 b\left(\frac{r}{\xi_r}; \Sigma, P(F)\right), \qquad (3)$$

$$\tilde{f}_c = \sigma \tilde{F}_c(\Sigma, P(F)). \qquad (4)$$

To perform numerical simulations of Eq. (1), the system is discretized in the r direction with a step ξ_r and put on a strip of finite width L, with periodic boundary conditions. The external force is replaced by a parabolic driving centered at w and of curvature κ. We compute the first stable configuration $u_{st}(r; w)$ reached by a front initially prepared at $u(r) = -\infty$ for 1000 samples. This can be done efficiently using the algorithm proposed in [30], based on the Middleton theorems [31].

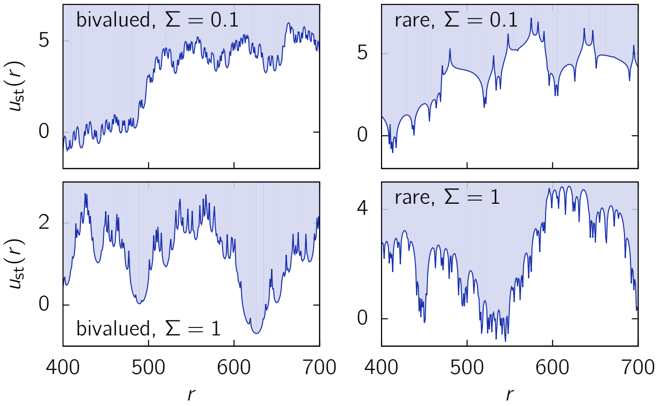

FIG. 2: (Color online) Stable front configurations for bivalued and rare disorder distributions and two values of the disorder parameter Σ. The fronts propagate upwards and the u coordinate has been shifted.

In each stable configuration, we compute the roughness of the line, defined by

$$B(\delta r) = \overline{\langle [u(r) - u(r+\delta r)]^2\rangle}, \qquad (5)$$

where $\overline{\cdot}$ is the average over disorder, and the pinning force $f_{st}(\kappa) = \kappa[w - \langle u_{st}(r; w)\rangle]$ where $\langle\cdot\rangle$ is the average over the position r. The critical force is then obtained with the formula $f_c = \overline{f_{st}(\kappa)} + c_1\sqrt{\kappa L \delta f_{st}^2} + \cdots$, where δf_{st} is the standard deviation of the pinning force distribution, used in the limit $\kappa \to 0$ and keeping $\kappa L \gg 1$. In this limit, $\sqrt{\kappa L \delta f_{st}^2} \sim \kappa^{1-\zeta}$ [32].

We used four different disorder distributions $P(F)$: bivalued, "rare" (with density $n = 0.1$) [34], Gaussian, and exponential. ξ_u is varied from 0.001 to 30 and σ from 1 to 8, and we set $c = 1$ and $\xi_r = 1$. The parabolic driving force is used as a convenient intermediary tool for the simulations, and has no noticeable effect in the limit $\kappa \to 0$.

Examples of stable front configurations are shown in Fig. 2, for bivalued and rare disorder distributions. At strong disorder ($\Sigma = 1$), the configurations look similar but the front amplitude is larger for the rare distribution. On the other hand, at weak disorder ($\Sigma = 0.1$), the configurations look very different but, contrary to the previous case, their amplitudes are the same.

The corresponding roughness functions are given in Fig. 3. For a strong disorder, the roughness is much higher for a rare disorder than for a bivalued disorder: this agrees with the direct observation of the fronts. For a weak disorder, the roughness does not seem to depend

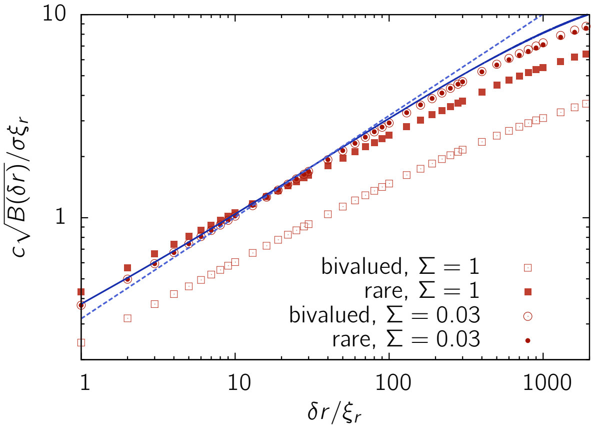

FIG. 3: (Color online) Crack front roughness: comparison between a bivalued (open symbols) and a rare distribution (full symbols), for weak (circles) and strong (squares) disorder. The solid line is the prediction using Larkin's approximation and the dashed line the long distance approximation [Eq. (7)].

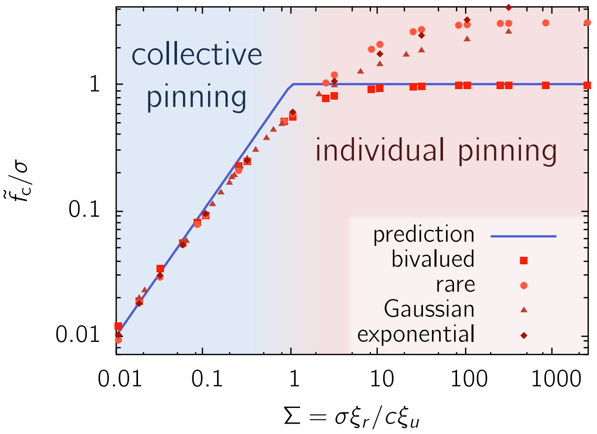

FIG. 4: (Color online) Disorder induced toughening: The net failure load $\tilde{f}_c$ is shown for different disorder distributions as a function of the disorder parameter Σ. The line shows the prediction of Eq. (10).

on the disorder distribution $P(F)$. The difference in the front shape is not seen in the roughness; this is not surprising since the roughness, as a two-point correlation function, cannot give a complete account of the front shape.

The disorder induced toughening (or net critical force) $\tilde{f}_c = f_c - \langle f \rangle$ is plotted versus the disorder parameter Σ on Fig. 4; and two regimes can be distinguished. At weak disorder ($\Sigma < 1$), we observe a beautiful collapse between different disorder distributions: this is the *collective pinning* regime. The net critical force follows the phenomenological law

$$\tilde{f}_c \simeq \frac{\sigma^2 \xi_r}{c \xi_u} = \sigma\Sigma; \tag{6}$$

that will be justified later by simple arguments. On the contrary, at strong disorder ($\Sigma > 1$), the critical force depends strongly on the disorder distribution: we are in the *individual pinning* regime.

In the limit $\Sigma \to \infty$, that can be interpreted as the limit $c \to 0$, the front is softer and has access to more and more disorder realizations. It may thus "choose" the more pinning one. As a result, when the disorder is bounded, the net critical force gets close to the maximum of the distribution. It is indeed what is observed for the bivalued distribution, whose maximum is 1, and for the "rare" distribution, whose maximum is $1/\sqrt{n} \simeq 3.16$. If the disorder is not bounded, the critical force is likely to diverge, as observed in the simulations. The fatter the distribution tail is, the faster the divergence is expected, that is also what is observed: the divergence is faster for the exponential distribution than for the Gaussian one.

We now show that simple arguments adapted from the Larkin and Ovchinnikov study of vortex pinning in superconductors [33] allow for an intuitive interpretation of our results. The main difficulty in dealing with Eq. (1) is its non linearity coming from the disorder term. The first Larkin assumption is that this difficulty can be circumvented at *short distances*, where the crack front does not see that the disorder correlation length ξ_u is finite. The Larkin model is thus defined as the limit $\xi_u = \infty$ (i.e. $\Sigma = 0$), that amounts of removing the u dependence of the disorder: $f(r,u) \to f(r)$. The propagation equation (1) is thus linear and admits a unique stable solution, that can be determined analytically. This gives, after an average over disorder, an exact expression for the roughness. In the limit $L \to \infty$ and $\kappa \to \infty$, and at long distances $r \gg \xi_r$, it takes the form

$$B(\delta r) \sim \left(\frac{\sigma \xi_r}{c}\right)^2 \frac{\delta r}{\xi_r}. \tag{7}$$

The exact expression and this approximation do not depend on the disorder distribution but only on its second moment σ^2.

The exact Larkin roughness and its limiting law (7) are compared to the simulations on Fig. 3. The agreement between the weak disorder simulations and the Larkin prediction is strikingly good. The long distance approximation is also rather good. On the contrary, strong disorder results are far from the prediction; that was expected since the prediction corresponds to $\Sigma = 0$.

We can address the question of the validity of the Larkin regime: what does the assumption of "short distances" mean? The answer involves the roughness that depicts the amplitude of the front perturbations at different scales. If these perturbations are smaller than the correlation length ξ_u, the Larkin model should represents correctly the behaviour of the line; on the contrary, when they are larger than ξ_u, a different behaviour is expected. This defines the length in the r direction up to which the

Larkin approximation is relevant, the so-called *Larkin length* L_c, by

$$\sqrt{B(L_\mathrm{c})} = \xi_u. \tag{8}$$

If the Larkin length is larger than the correlation length ξ_r, its expression can be derived from Eq. (7):

$$L_\mathrm{c} = \left(\frac{c\xi_u}{\sigma\xi_r}\right)^2 \xi_r = \frac{\xi_r}{\Sigma^2}. \tag{9}$$

The domains of size L_c that behave as if ξ_u was infinite are called *Larkin domains.*

To predict the external force required to unpin the line, we compute the average resistance seen by a domain of size L_r in the Larkin model. This resistance has a mean $\langle f\rangle$ and its standard deviation depends on L_r: if $L_r < \xi_r$, the domain sees only one defect and the standard deviation is σ; if $L_r > \xi_r$, the front averages the local toughness over L_r/ξ_r uncorrelated defects and the standard deviation is $\sigma\sqrt{\xi_r/L_r}$. This is valid up to $L_r = L_\mathrm{c}$, where the Larkin model breaks down. Beyond that scale, the important wandering of the crack front results in correlations of the local toughness actually experienced by the system. The second Larkin assumption is that the critical force is given by the typical toughness seen by a Larkin domain; this leads to two cases:

- if $L_\mathrm{c} > \xi_r$ (or $\Sigma < 1$), a Larkin domain sees several defects: this is the *collective pinning* regime, where the net critical force is $\tilde{f}_\mathrm{c} = \sigma\sqrt{\xi_r/L_\mathrm{c}}$.
- if $L_\mathrm{c} < \xi_r$ (or $\Sigma > 1$), a Larkin domain sees only one defect: we are in the *individual pinning* regime. The net critical force is now $\tilde{f}_\mathrm{c} = \sigma$.

Using the long distance expression of the Larkin length (7), we can write explicitly the net critical load,

$$\tilde{f}_\mathrm{c} = \begin{cases} \dfrac{\sigma^2\xi_r}{c\xi_u} = \sigma\Sigma & \text{if } \Sigma = \dfrac{\sigma\xi_r}{c\xi_u} < 1, \\ \sigma & \text{if } \Sigma = \dfrac{\sigma\xi_r}{c\xi_u} > 1. \end{cases} \tag{10}$$

These expressions are compared to the simulations in Fig. 4 for the four different disorder distributions. In the collective pinning regime, the prevision captures the results of the simulations: this confirms the validity of Eq. (6), irrespective of the underlying local toughness distribution. The effective toughness, that is a priori a non-universal quantity, is shown here to be remarkably robust.

In the individual pinning regime, the prediction (10) does not account for all the investigated materials, but provides a lower-bound of the effective toughness, as is seen in Fig. 4. Indeed, the pinning process filters the local toughness distribution towards strong defects of resistance $f \geq \sigma$.

Since the elastic constant of the front is given by the critical force, Eq. (6) for the collective regime is actually an implicit equation for f_c, whose solution is

$$f_\mathrm{c} = \frac{1}{2}\left(\langle f\rangle + \sqrt{\langle f\rangle^2 + 4\frac{\sigma^2\xi_r}{\xi_u}}\right). \tag{11}$$

It follows that the disorder parameter satisfies $\Sigma \leq \sqrt{\xi_r/\xi_u}$; this notably implies that the individual pinning regime is only accessible to anisotropic materials. The expression above represents a powerful tool to design the microstructure of composites in order to achieve improved failure properties.

To conclude, we have shown that the interaction between the front of a brittle crack and a disordered microstructure is governed by one dimensionless parameter and that two distinct regimes can be identified. In the collective pinning regime that occurs at low disorder strength, many impurities act together to pin the crack front. These impurities are averaged and give rise to an effective toughness given by Eq. (6), that depends on a few parameters measurable from the material microstructure. On the other hand, at high disorder strength, the front is pinned by strong individual defects: this is the individual pinning regime. The basic quantities studied here are shown to depend on many parameters, such as the disorder distribution. This has a negative effect on the predictability of systems falling in this regime, but it might be used advantageously for the design of composites with improved toughness. Notably, our study shows that a few but strong impurities produce a larger toughening than a large number of weak ones.

The authors would like to thank J.-B. Leblond, V. Lecomte, N. Pindra and S. Roux for very helpful discussions.

---

[*] Electronic address: vincent.demery@polytechnique.edu
[†] Electronic address: laurent.ponson@upmc.fr
[‡] Electronic address: alberto.rosso@lptms.u-psud.fr

[1] D. Bonamy and E. Bouchaud, Phys. Rep. **498**, 1 (2011).
[2] S. Zaperri, P. Cizeau, G. Durin, and H. E. Stanley, Phys. Rev. E **58**, 6353 (1998).
[3] S. Lemerle, J. Ferré, C. Chappert, V. Mathet, T. Giamarchi, and P. Le Doussal, Phys. Rev. Lett. **80**, 849 (1998).
[4] A. I. Larkin and Y. N. Ovchinnikov, *Nonequilibrium superconductivity* (Elsevier, 1989).
[5] E. Vives, J. Ortin, L. Manosa, I. Rafols, R. Perezmagrane, and A. Planes, Phys. Rev. Lett. **72**, 1694 (1994).
[6] W. D. Callister, *Fundamentals of materials science and engineering* (Wiley & Sons., 2012).
[7] S. Roux, D. Vandembroucq, and F. Hild, Eur. J. Mech. A **22**, 743 (2003).
[8] S. Roux and F. Hild, Int. J. Frac. **166**, 154 (2008).
[9] S. Xia, L. Ponson, G. Ravichandran, and K. Bhattacharya, Phys. Rev. Lett. **108**, 196101 (2012).

[10] H. Gao and J. R. Rice, J. Appl. Mech. **56**, 828 (1989).

[11] J. Schmittbuhl, S. Roux, J. P. Vilotte, and K. J. Måløy, Phys. Rev. Lett. **74**, 1787 (1995).

[12] L. Ponson and D. Bonamy, Int. J. Frac. **162**, 21 (2010).

[13] J. R. Rice, Journal of Applied Mechanics **52**, 571 (1985).

[14] J. F. Joanny and P. G. d. Gennes, The Journal of Chemical Physics **81**, 552 (1984).

[15] P. L. Doussal, K. J. Wiese, E. Raphael, and R. Golestanian, Phys. Rev. Lett. **96**, 015702 (2006).

[16] M. V. ad J.B. Leblond and L. Ponson, Int. J. Solids Struct. **50**, 371 (2013).

[17] P. J. Metaxas, J. P. Jamet, A. Mougin, M. Cormier, J. Ferré, V. Baltz, B. Rodmacq, B. Dieny, and R. L. Stamps, Phys. Rev. Lett. **99**, 217208 (2007).

[18] P. G. D. Gennes, Rev. Mod. Phys. **57**, 827 (1985).

[19] S. Moulinet, C. Guthmann, and E. Rolley, The European Physical Journal E **8**, 437 (2002), ISSN 1292-8941.

[20] S. Moulinet, A. Rosso, W. Krauth, and E. Rolley, Phys. Rev. E **69**, 035103 (2004).

[21] E. Agoritsas, V. Lecomte, and T. Giamarchi, Physica B: Condensed Matter (2012), ISSN 0921-4526.

[22] D. S. Fisher, Phys. Rev. B **31**, 1396 (1985).

[23] T. Nattermann, S. Stepanow, L.-H. Tang, and H. Leschhorn, J. Phys. II France **2**, 1483 (1992).

[24] O. Narayan and D. S. Fisher, Phys. Rev. B **48**, 7030 (1993).

[25] P. Le Doussal, K. J. Wiese, and P. Chauve, Phys. Rev. B **66**, 174201 (2002).

[26] S. Bustingorry, A. B. Kolton, and T. Giamarchi, EPL (Europhysics Letters) **81**, 26005 (2008).

[27] D. Bonamy, S. Santucci, and L. Ponson, Phys. Rev. Lett. **101**, 045501 (2008).

[28] L. Ponson, Phys. Rev. Lett. **103**, 055501 (2009).

[29] S. Santucci, M. Grob, R. Toussaint, J. Schmittbuhl, A. Hansen, and K. J. Maloy, Eur. Phys. J. **92**, 44001 (2010).

[30] A. Rosso and W. Krauth, Phys. Rev. E **65**, 025101 (2002).

[31] A. A. Middleton, Phys. Rev. Lett. **68**, 670 (1992).

[32] A. Rosso, P. Le Doussal, and K. J. Wiese, Phys. Rev. B **75**, 220201 (2007).

[33] A. I. Larkin and Y. N. Ovchinnikov, Journal of Low Temperature Physics **34**, 409 (1979), ISSN 0022-2291, 10.1007/BF00117160.

[34] The rare distribution with a density n is defined by $P_{\mathrm{rare},n}(F) = \frac{n}{2}\left[\delta\left(F+\frac{1}{\sqrt{n}}\right)+\delta\left(F-\frac{1}{\sqrt{n}}\right)\right]$.